Orientational Coherent Effects of High-Energy Particles in a $LiNbO_3$ Crystal

E. Bagli, V. Guidi, A. Mazzolari, L. Bandiera, G. Germogli, and A. I. Sytov
INFN Sezione di Ferrara, Dipartimento di Fisica e Scienze della Terra, Università di Ferrara Via Saragat 1, 44100 Ferrara, Italy

D. De Salvador, A. Argiolas, M. Bazzan, and A. Carnera
Dipartimento di Fisica e Astronomia, Università di Padova, Via Marzolo 8, 35131 Padova, Italy and INFN Laboratori Nazionali di Legnaro, Viale dell'Università 2, 35020 Legnaro, Italy

A. Berra, D. Bolognini, D. Lietti, and M. Prest
Università dell'Insubria, via Valleggio 11, 22100 Como, Italy and INFN Sezione di Milano Bicocca, Piazza della Scienza 3, 20126 Milano, Italy

E. Vallazza
INFN Sezione di Trieste, Via Valerio 2, 34127 Trieste, Italy
(Received 20 February 2015; published 2 July 2015)

A bent lithium niobate strip was exposed to a 400-GeV/c proton beam at the external lines of CERN Super Proton Synchrotron to probe its capabilities versus coherent interactions of the particles with the crystal such as channeling and volume reflection. Lithium niobate ($LiNbO_3$) exhibits an interplanar electric field comparable to that of Silicon (Si) and remarkable piezoelectric properties, which could be exploited for the realization of piezo-actuated devices for the control of high-energy particle beams. In contrast to Si and germanium (Ge), $LiNbO_3$ shows an intriguing effect; in spite of a low channeling efficiency (3%), the volume reflection maintains a high deflection efficiency (83%). Such discrepancy was ascribed to the high concentration (10^4 per cm^2) of dislocations in our sample, which was obtained from a commercial wafer. Indeed, it has been theoretically shown that a channeling efficiency comparable with that of Si or Ge would be attained with a crystal at low defect concentration (less than ten per cm^2). To better understand the role of dislocations on volume reflection, we have worked out computer simulation via DYNECHARM++ Monte Carlo code to study the effect of dislocations on volume reflection. The results of the simulations agree with experimental records, demonstrating that volume reflection is more robust than channeling in the presence of dislocations.

DOI: 10.1103/PhysRevLett.115.015503 PACS numbers: 61.85.+p, 29.27.-a

Channeling manifests itself as a charged particle impinges on crystal planes at an angle lower than the critical angle for channeling [1]. In 1976, Tsyganov proposed the use of bent crystals in order to manipulate charged particles trajectories [2,3]. In fact, crystalline planes can trap (channeling) or reflect (volume reflection) charged particles. Recently, a significant boost for the research on particle-crystal interactions was provided by the fabrication of uniformly bent crystals [4,5] with suitable thickness along the beam [6,7]. Coherent interactions proved the capability of manipulating positively [8–11] and negatively [12–17] charged particle beams from MeV energies [18] up to hundreds of GeV. Orientational effects were exploited for steering [19], collimation [20–23], and extraction [21,24–26] of relativistic charged beams in circular accelerators, as well as splitting and focusing of extracted beams [27], leading to the installation of two bent crystal devices in the Large Hadron Collider (LHC) for collimation purposes [28].

Silicon (Si) has always been the key material for the exploitation of coherent interactions, thanks to the large availability of starting material with low defect concentration (less than ten per cm^2). The concentration of dislocations is traditionally referred to the length of dislocation lines by unit volume, i.e., for randomly distributed dislocations, the areal density of dislocations intercepted by a random plane. Germanium (Ge), the natural alternative to Si, demonstrated an ability to overcome the performances of Si owing to its deeper potential well [29–31]. However, particular care is needed in the selection of starting material in terms of defect concentration. Recently, coherent effects at high energy in a self-bent graded $Si_{1-x}Ge_x$ crystals were observed [32]. The intrinsic curvature of such systems would restrain the detrimental impact of any mechanical bending device. However, the presence of $\sim 10^2$ dislocations per cm^2 induced by the growth process reduces the deflection efficiency for channeling to 62.5% against the predicted 76.5%, while leaving almost unaltered the efficiency for volume reflection at 96.0% [32].

A promising crystalline material for the manipulation of particle beams via coherent interaction is $LiNbO_3$. This material is widely used in photonic industry and is nowadays available in large wafers for optical applications. The potential advantage of such material for the exploitation of coherent effects is twofold: (i) its average atomic number (13.6) comparable to that of Si (14) and (ii) its remarkable piezoelectric properties [33], which could be exploited for the manipulation of its geometry. As an example, the crystal-based schemes for ongoing collimation experiment at high energy makes use of statically bent crystals operating under ultrahigh vacuum [22]. The usage of a piezo-actuated crystal would allow fine tuning of the radius of curvature. For such a case, two electrodes deposited on the opposite surface as that exposed to the beam would impart the desired deformation (see video at [34] for lively understanding of the dynamical deformation of the crystalline planes and related Supplemental Material at [34], which includes Ref. [35]). In the same application, a set of four electrodes would also compensate for the torsion induced by the mechanical holder. As a second application, an alternate pattern of electrodes on the two main surfaces of a crystal could impart a undulating shape to the $LiNbO_3$, leading to the design of innovative x- and γ-ray sources [36].

In this Letter, the orientational effects of 400-GeV/c protons interacting with a $LiNbO_3$ crystal protons are studied. The experiments were carried out at the H8 CERN-SPS extracted line.

$LiNbO_3$ possesses trigonal crystalline structure. In the conventional hexagonal representation, the basal lattice vectors are equally long and are separated by a 120° angle, and the third axis is directed along the polar (ferroelectric) axis. It is customary to define three orthoexagonal directions (X, Y, Z) identifying three set of planes, perpendicular to the $(11\bar{2}0)$, the $(\bar{1}100)$, and the (0001) directions, respectively. Figure 1(b) shows the structure of the $LiNbO_3$ cell with the Y planes highlighted. In Fig. 1(c), the Coulombic potential of the Y planes of $LiNbO_3$ and of the (110) planes of Si and Ge is compared.

A strip crystal was manufactured starting from commercially available $LiNbO_3$ wafers (Crystal. Tech. Inc.). The wafers were free of stacking fault and cluster defects, but they present point defects and dislocations, i.e., a defect for which an extra plane is inserted in the atomic structure [38]. The starting material was extensively characterized before the exposure to the high-energy beam. Preliminary Rutherford Backscattering (RBS)-channeling analyses were performed at the 2-MeV proton beam provided by AN2000 accelerators of INFN-LNL, assessing the Y plane as the most efficient under channeling. A portion of the starting wafer was analyzed via etch-pits density technique, and a $N_d = 10^4$ per cm^2 dislocation density was assessed

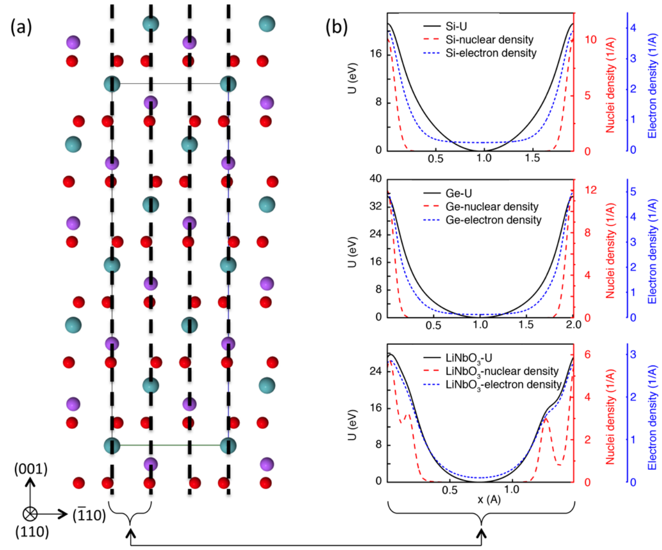

FIG. 1 (color online). (a) Etch-pitch density analysis of a portion of the $LiNbO_3$ starting wafer. (b) Sketch of the $LiNbO_3$ unit cell. The Li atoms are shown in purple, the Nb in green, and the O in red. The channeling Y planes are highlighted. (c) The potential, electron, and nuclei density for Si (110), Ge (110), and $LiNbO_3$ Y planes evaluated through the ECHARM software [37].

[see Fig. 1(a) and Ref. [39]], a concentration compatible with the usage for optical purposes [40].

The strip crystal had sizes of $0.9 \times 1.0 \times 70.0$ mm^3 and was bent by means of a standard mechanical device [41], imparting a primary curvature around the Z axis. Therefore, the 1.0-mm-long Y planes are subjected to anticlastic deformation [4,26], resulting in a bending radius of 5.46 m. Different from the Si and Ge (110) planes, the $LiNbO_3$ Y plane exhibits an asymmetric potential well. Thus, the bending radius was purposely chosen directed along the negative Y axis in order to concentrate the particle trajectories far from the zone with high concentration of nuclei [see Fig. 1(c)].

The strip was exposed to a 400-GeV/c proton beam at the H8 CERN-SPS extracted line. Beam size rms was 0.19×0.84 mm^2 and divergence rms 11.47×9.44 μrad^2. The strip faces parallel to the Y planes were aligned with the beam direction. The holder with the strip was mounted on a two-axis goniometer with ~1-μrad angular resolution. The particle incoming and outgoing angles from the crystal were detected via a telescope system, with ~3.5-μrad angular resolution [42]. A detailed description of the experimental setup can be found in Ref. [43].

Figure 2(a) shows the distribution of the deflection angle of the particles after interaction with the crystal as a function of the entrance angle. Figures 2(a) and 2(b) sketch the most relevant mechanisms of interaction of a charged particle with a bent crystal. Under channeling (1), particles with a transverse energy lower than the potential well depth are captured and deflected by the crystal bending angle.

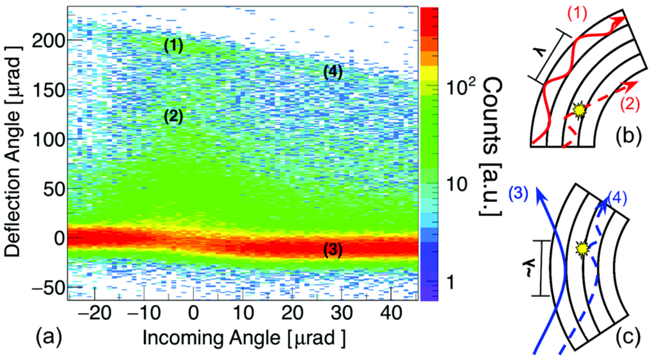

FIG. 2 (color online). (a) Distribution of the deflection angle of the particles after the interaction with the $LiNbO_3$ strip as a function of the particle incoming angle with respect to the channeling plane. (b) Scheme of the channeling (1) and the dechanneling (2) mechanisms. (c) Scheme of the volume reflection (3) and the volume capture (4) mechanisms.

Because of multiple scattering, channeled particles may suffer dechanneling (2) [14,44,45], lowering the steering efficiency. On the other hand, volume reflection (3) manifests whenever a particle trajectory becomes tangent to bent atomic planes [8,12,46]. Because a particle can lose transverse energy during the interaction, the reflected particles may undergo volume capture (4) [47], being captured under channeling.

Figure 3 shows the distribution of particle deflection angles after the interaction with the crystals for channeling and volume reflection orientations. For the channeling case, a fraction of $3\% \pm 1\%$ of the beam is deflected by the nominal bending angle (190 ± 3 μrad), in contrast to what was obtainable with a Si (66%) [11] or a Ge (72%) [30] strip of the same geometrical properties. The deflection efficiency of channeling and volume reflection and the statistical error are calculated according to Ref. [48]. The dechanneling length, i.e., the length for which a $1/e$ fraction of the initially channeled particles have left the channeling state, was measured to be 0.35 mm, lower than 1.5 mm for Si [45]. As the crystal was oriented in order to excite volume reflection, most of the particles ($83\% \pm 2\%$) were deflected at an angle of 11.9 ± 0.5 μrad, comparable to Si (97.5% and 11.7 μrad) [9] and Ge (96.6% and 17.3 μrad) [30]. The lower value for the dechanneling length suggests that the particle trajectories are largely altered by the presence of dislocations in the $LiNbO_3$.

Currently available $LiNbO_3$ crystals exhibit a high deflection efficiency under volume reflection condition. By properly aligning a series of crystal strips under such condition [49], repeated reflections add up without significant efficiency degradation [10]. The reciprocal alignment of the strips is demanded to be less than a few tens of μrad using a limited amount of space [50]. The usage of static holders exhibits scarce reproducibility of the reciprocal alignment of the strips. A series of $LiNbO_3$ strips mounted on a static holder can overcome such limitation by exploiting the piezoelectric effect to obtain the fine alignment of each strip. Therefore, the $LiNbO_3$ would be an ideal crystal for the fabrication of a dynamic and compact series of strips (see Supplemental Material for the simplest case of a single strip piezo-actuated crystal).

The maintenance of piezo-electric properties versus irradiation is expected for relativistic particles. In fact, the influence of radiation damage on the polar properties of $LiNbO_3$ has been explored in the low-energy regime (~100 keV up to 22 MeV) with different ions [51] at fluences ranging from 10^{14} to 10^{16} atoms per cm^2. A significant degradation of polarization-related properties was observed only for strong lattice amorphization ($> 10\%$ of disordered fraction), which should not be attained at relativistic energies. Besides piezo-electricity, coherent effects have been shown to survive versus radiation damage. Radiation generates pointlike defects, which negligibly affect the channeling efficiency ($\ll 0.01\%$) [52–54]. Indeed, the number of pointlike defects has to be a part per mill of the total number of atoms in the crystal to spoil coherent effects [54,55]. For instance, Si was proven to be radiation hard for channeling with 450-GeV/c protons during a full year of continuous operations to a peak fluence of 5×10^{20} particles per cm^2 [56], a value by far larger than 2.2×10^{14} integrated intensity in the LHC in 2012 [57].

In order to provide an insight into the influence of defects on channeling and volume reflections, a Monte Carlo simulation was worked out via DYNECHARM++ code [58], which incorporates a subroutine to account for the presence of crystal defects [55]. Defects can be grouped according to their dimensionality in the lattice on which they act, i.e., pointlike (interstitial atoms and vacancies), linear (dislocations), two-dimensional (stacking faults), and three-dimensional (amorphous clusters) defects [52]. Because pointlike defects negligibly affect the channeling efficiency, they were not considered in the simulation. Moreover, etch-pitch density measurements showed no evidence of stacking faults; thereby simulations were performed by assuming dislocations as the sole structural defects. Measured beam parameters and N_d were used as inputs. The types of dislocation in the $LiNbO_3$ crystal were described according to Ref. [59].

By setting a concentration of 0.7×10^4 defects per cm^2, the simulation allowed obtaining a deflection efficiency of ~3% and ~80% under channeling and volume reflection, respectively, in agreement with the experimental results and the measured dislocation concentration. Then a $LiNbO_3$ crystal with a N_d comparable to that of Si and Ge (< 10 per cm^2) was studied through Monte Carlo simulations. Such a crystal corresponds to a realistic situation, which could be produced via special techniques [60]. Simulated deflection efficiencies were $68\% \pm 1\%$ for channeling and $94\% \pm 1\%$ for volume reflection, fully in line with those of Si (66% and 97.5%) and Ge (72% and 96.6%). The dechanneling length for this crystal was

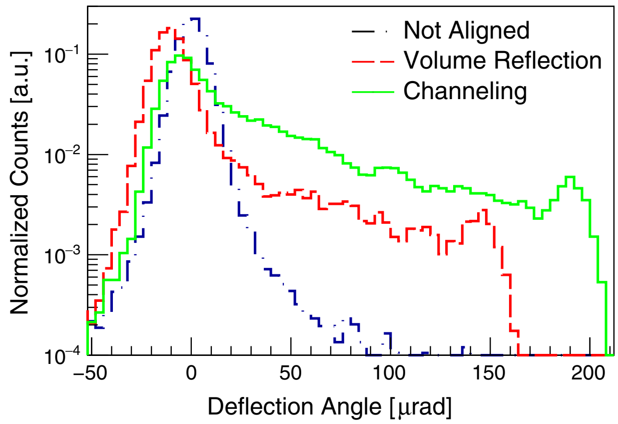

FIG. 3 (color online). Beam profiles as the crystal is randomly aligned to a 400 GeV/c proton beam (blue dash-dotted line), under channeling condition (green continuous line) and under volume reflection condition (red dashed line).

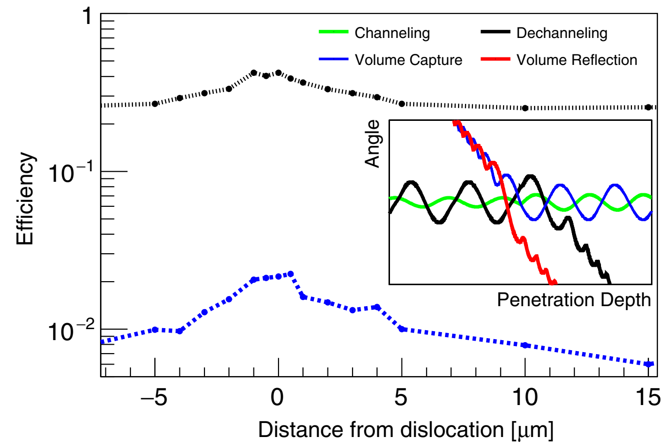

FIG. 4 (color online). Efficiency of dechanneling and volume capture process for a 400-GeV/c proton beam interacting with a bent Si (110) crystal. The inset shows the evolution of the angles for four particles interacting with a edge dislocation centered on the axis origin. The reference frame used is noninertial. The inset allows one to observe that the two trajectories are time reversed, as they are linked by the Lindhard reversibility rule [1].

0.95 ± 0.05 mm, i.e., approximately three times greater than the measured level 0.35 mm and close to the 1.5 mm for Si.

Since the presence of dislocations in the $LiNbO_3$ crystal was ascribed to be responsible for the degradation of deflection efficiencies of coherent effects at high energy, its study deserves a thorough investigation. Indeed, the detrimental effect of their presence on channeling at high energy was already extensively discussed in Ref. [54]. In contrast, their influence on volume reflected particles has never been dealt with in detail.

Let us analyze at the microscopic level four usual processes a particle may incur in a bent crystal, i.e., channeling, dechanneling, volume reflection, and volume capture (see inset of Fig. 4). The dechanneling and volume capture processes (the competitive processes of channeling and volume reflection, respectively) usually occur due to incoherent scattering with nuclei or electrons. A dechanneled particle "acquires" enough transverse energy to leave the channeling state, while a volume-captured particle "loses" enough energy to be captured under channeling condition. In the case that incoherent scattering is neglected, the cases of volume capture and dechanneling are prevented. We ran a simulation by neglecting incoherent scattering for a crystal with a dislocation and observed some trajectories for volume captured and dechanneled particles. In fact, the displacement field due to a dislocation modifies the potential, causing a variation of the transverse energy, which may force the particle to dechannel or to be volume captured.

Crystals usually contain dislocation lines that lay on the major cleavage planes, i.e., the "weakest" planes in a crystal. For $LiNbO_3$ they are $(01\bar{1}2)$, $(1\bar{1}02)$, and $(\bar{1}012)$. The typical dislocation in a $LiNbO_3$ is neither pure edge nor pure screw [59]. In order to investigate the quantitative influence of dislocations on volume reflection, let us consider a simpler case for which the effect of dislocations on channeling efficiency has already been studied [54], i.e., a Si (110) crystal. Although Si and $LiNbO_3$ exhibit two different crystalline symmetries, the dynamics of channeled particles is solely determined by the shape of the potential well under the continuum approximation, which are very much alike for the two crystals (see Fig. 1).

Figure 4 shows the efficiency of dechanneling and volume capture, i.e., the inefficiency of channeling and volume reflection, respectively, as a function of the minimum distance of a trajectory from the dislocation. The data are simulated for a collimated 400 GeV/c proton beam, interacting with a Si (110) crystal with the same geometrical parameters as for the $LiNbO_3$ strip and a single-edge dislocation randomly distributed in the crystal. The result of the simulation allows one to better perceive the "robustness" of volume reflection with respect to channeling in the presence of a dislocation. Transversely, the coherent effects are affected within $\pm 20\ \mu$m far from the dislocation, in agreement with the literature [54].

The average loss of efficiencies for the two processes is rather constant in the vicinity of the dislocation, mainly during a particle oscillation period (λ). For volume reflection, such a condition holds only over a length of the order of λ, where the reflection occurs (see Fig. 2). In contrast, for channeling, the particle oscillates between two adjacent planes all over the whole crystal length L. As a consequence, volume capture probability is proportional to λN_d, while dechanneling to LN_d. Bearing in mind that the two processes are the time reversal processes of each other [1], their probability proportionality constants are equal. As a result, the ratio of their efficiencies owing to dislocations has to be $\propto L/\lambda$. In our particular case, the ratio is $1\ \mathrm{mm}/60\ \mu\mathrm{m} \sim 16$ in agreement with the average ratio ~ 12 obtained by the simulations (see Fig. 4). In summary, the robustness of the volume reflection is due to the shorter length over which the coherent process must occur.

Moreover, the efficiency curves in Fig. 4 are slightly asymmetric. Indeed, the displacement field of an edge dislocation impresses a local curvature to the crystalline planes on both directions and symmetrically with respect to the extra plane of the dislocation. In contrast, the global curvature goes toward only one direction. Therefore, when the effect of the two curvatures sums up with the same sign, the probability for volume capture decreases [9] and for dechanneling increases [11]. The opposite effect occurs when the two curvatures have opposite signs.

In summary, coherent effects in a bent piezoelectric $LiNbO_3$ crystal with $\sim 10^4$ dislocations per cm^2 have been experimentally observed. The efficiency of deflection under channeling is limited by the high-dislocation density of commercially available wafers, while under volume reflection, efficiency is not significantly affected, making possible its exploitation for operation at high energy via the multivolume reflection scheme. Monte Carlo simulations were worked out by taking into account the influence of dislocations to the particle trajectories. Simulations showed that dislocations increase the probability of dechanneling and volume capture; i.e., they spoil the steering efficiency for channeling and volume reflection, respectively.

We acknowledge M. Gelain and S. Carturan of LNL for help in dislocation etch pits density measurements. We acknowledge partial support by INFN under the CHANEL project.

[1] J. Lindhard, K. Dan. Vidensk. Selsk. Mat. Fys. Medd. **34**, 14 (1965).
[2] E. Tsyganov, Some aspects of the mechanism of a charge particle penetration through a monocrystal. Fermilab Technical Report, preprint TM-682 (1976).
[3] E. Tsyganov, Estimates of cooling and bending processes for charged particle penetration through a mono crystal, Fermilab Technical Report, preprint TM-684 (1976).
[4] V. Guidi, L. Lanzoni, and A. Mazzolari, J. Appl. Phys. **107**, 113534 (2010).
[5] Y. Ivanov, A. Petrunin, and V. Skorobogatov, J. Exp. Theor. Phys. Lett. **81**, 99 (2005).
[6] V. Guidi, A. Antonini, S. Baricordi, F. Logallo, C. Malag, E. Milan, A. Ronzoni, M. Stefancich, G. Martinelli, and A. Vomiero, Nucl. Instrum. Methods Phys. Res., Sect. B **234**, 40 (2005).
[7] A. Mazzolari, V. Guidi, D. D. Salvador, and L. Bacci, Nucl. Instrum. Methods Phys. Res., Sect. B **309**, 130 (2013).
[8] W. Scandale *et al.*, Phys. Rev. Lett. **98**, 154801 (2007).
[9] W. Scandale *et al.*, Phys. Rev. Lett. **101**, 234801 (2008).
[10] W. Scandale *et al.*, Phys. Lett. B **688**, 284 (2010).
[11] E. Bagli, L. Bandiera, V. Guidi, A. Mazzolari, D. Salvador, A. Berra, D. Lietti, M. Prest, and E. Vallazza, Eur. Phys. J. C **74**, 2740 (2014).
[12] W. Scandale *et al.*, Phys. Lett. B **681**, 233 (2009).
[13] W. Scandale *et al.*, Phys. Lett. B **680**, 301 (2009).
[14] W. Scandale *et al.*, Phys. Lett. B **719**, 70 (2013).
[15] A. Mazzolari, E. Bagli, L. Bandiera, V. Guidi, H. Backe, W. Lauth, V. Tikhomirov, A. Berra, D. Lietti, M. Prest, E. Vallazza, and D. De Salvador, Phys. Rev. Lett. **112**, 135503 (2014).
[16] W. Lauth, H. Backe, P. Kunz, and A. Rueda, Int. J. Mod. Phys. A **25**, 136 (2010).
[17] U. Wienands *et al.*, Phys. Rev. Lett. **114**, 074801 (2015).
[18] V. Guidi, A. Mazzolari, D. De Salvador, and L. Bacci, Phys. Rev. Lett. **108**, 014801 (2012).
[19] A. F. Elishev *et al.*, Phys. Lett. B **88**, 387 (1979).
[20] R. P. Fliller, A. Drees, D. Gassner, L. Hammons, G. McIntyre, S. Peggs, D. Trbojevic, V. Biryukov, Y. Chesnokov, and V. Terekhov, Nucl. Instrum. Methods Phys. Res., Sect. B **234**, 47 (2005).
[21] A. G. Afonin *et al.*, Phys. Rev. Lett. **87**, 094802 (2001).
[22] W. Scandale *et al.*, Phys. Lett. B **692**, 78 (2010).
[23] N. Mokhov, G. Annala, A. Apyan *et al.*, *Proceedings of the 23rd Particle Accelerator Conference (PAC'09), Vancouver, BC, Canada, 2009* (Triumf, Vancouver, 2010), p. WE1GRC05.
[24] R. A. Carrigan *et al.*, Phys. Rev. ST Accel. Beams **5**, 043501 (2002).
[25] H. Akbari *et al.*, Phys. Lett. B **313**, 491 (1993).
[26] A. G. Afonin *et al.*, J. Exp. Theor. Phys. Lett. **67**, 781 (1998).
[27] A. S. Denisov *et al.*, Nucl. Instrum. Methods Phys. Res., Sect. B **69**, 382 (1992).
[28] W. Scandale *et al.*, CERN Report No. CERN-LHCC-2011-007; LHCC-I-019, 10 June, 2011.
[29] D. De Salvador *et al.*, Appl. Phys. Lett. **98**, 234102 (2011).
[30] D. De Salvador *et al.*, J. Appl. Phys. **114**, 154902 (2013).
[31] D. De Salvador *et al.*, AIP Conf. Proc. **1530**, 103 (2013).
[32] E. Bagli *et al.*, Phys. Rev. Lett. **110**, 175502 (2013).
[33] R. Weis and T. Gaylord, Appl. Phys. A **37**, 191 (1985).
[34] See Supplemental Material at http://link.aps.org/supplemental/10.1103/PhysRevLett.115.015503 for a possible scheme to impart a controlled deformation to a $LiNbO_3$ strip crystal by depositing a electrode pattern on its surface and applying an appropriate voltage.
[35] H. Ogi, Y. Kawasaki, M. Hirao, and H. Ledbetter, J. Appl. Phys. **92**, 2451 (2002).
[36] V. Baryshevsky, I. Dubovskaya, and A. Grubich, Phys. Lett. **77A**, 61 (1980).
[37] E. Bagli, V. Guidi, and V. A. Maisheev, Phys. Rev. E **81**, 026708 (2010).
[38] J. P. Hirth and J. Lothe, *Theory of Dislocations* (Wiley, New York, 1982), 2nd ed., Vol. 1.
[39] M. Gelain, Ottimizzazione di Cristalli di Niobato di Litio per Channeling di Particelle Relativistiche, Bachelor thesis, University of Padua, 2011.
[40] A. M. Prokhorov and Y. S. Kuz'minov, *Physics and Chemistry of Cristalline Lithium Niobate* (CRC Press, Bristol, New York, 1990).
[41] A. Mazzolari *et al.*, *Proceedings of 1st International Particle Accelerator Conference (IPAC'10), Kyoto, Japan, 2010*, eConf C100523, TUPEC080 (2010).
[42] S. Hasan, Experimental Techniques for Deflection and Radiation Studies with Bent Crystals, Ph.D. thesis, University of Insubria, 2011.

[43] L. Celano, D. Creanza, M. de Palma, G. Maggi, L. Fiore, V. Paticchio, G. Raso, G. Selvaggi, L. Silvestris, and P. Tempesta, Nucl. Instrum. Methods Phys. Res., Sect. A **381**, 49 (1996).
[44] V. M. Biryukov, Y. A. Chesnekov, and V. I. Kotov, *Crystal Channeling and Its Applications at High-Energy Accelerators* (Springer, Berlin, 1996).
[45] W. Scandale *et al.*, Phys. Lett. B **680**, 129 (2009).
[46] A. Taratin and S. Vorobiev, Phys. Lett. A **119**, 425 (1987).
[47] A. Taratin and S. Vorobiev, Nucl. Instrum. Methods Phys. Res., Sect. B **47**, 247 (1990).
[48] W. Scandale *et al.*, Phys. Rev. ST Accel. Beams **11**, 063501 (2008).
[49] W. Scandale *et al.*, Phys. Lett. B **658**, 109 (2008).
[50] E Bagli *et al.*, J. Instrum. **7**, P04002 (2012).
[51] F. Chen, J. Appl. Phys. **106**, 081101 (2009).
[52] L. Feldman, J. Mayer, and S. Picraux, *Materials Analysis by Ion Channeling* (Academic Press, London, 1982).
[53] S. I Baker, R. A. Carrigan, Jr., V. R. Cupps II, J. S. Forster, W. M. Gibson, and C. R. Sun, Nucl. Instrum. Methods Phys. Res., Sect. B **90**, 119 (1994).
[54] V. M. Biryukov, Phys. Rev. E **52**, 2045 (1995).
[55] E. Bagli and V. Guidi, Nucl. Instrum. Methods Phys. Res., Sect. B **355**, 365 (2015).
[56] A. Baurichter *et al.*, Nucl. Instrum. Methods Phys. Res., Sect. B **164–165**, 27 (2000).
[57] M. Lamont, J. Phys. Conf. Ser. **455**, 012001 (2013).
[58] E. Bagli and V. Guidi, Nucl. Instrum. Methods Phys. Res., Sect. B **309**, 124 (2013).
[59] Y. Okada and T. Iizuka, J. Appl. Crystallogr. **9**, 375 (1976).
[60] D.-H. Yoon, I. Yonenaga, T. Fukuda, and N. Ohnishi, J. Cryst. Growth **142**, 339 (1994).